

PILOT SEQUENCE DESIGN FOR SPACE-TIME CODED ARTM CPM

Willie Harrison, Michael Rice, Spencer Giddens, Chad Josephson

Department of Electrical and Computer Engineering

Brigham Young University

Provo, UT 84602

willie.harrison@byu.edu, mdr@byu.edu,

giddens2spencer@gmail.com, chadcjosephson@gmail.com

ABSTRACT

Solving the two-antenna problem for the ARTM CPM waveform requires optimal estimation for a number of unknown signal parameters at the receiver to enable a space-time block-coded solution. To accomplish the required parameter estimation, known pilot bit sequences are added to the data structure of the transmitter. The degree to which optimal detection may occur for these unknown parameters is a function of the specific pilot sequences chosen. This paper outlines the principles for designing the pilot sequences, lists the chosen sequences explicitly, and shows that the pilots achieve the lowest Cramér-Rao lower bounds in the estimators for several of the key parameters. These pilot sequences are to be used in implementations of space-time coded ARTM CPM aeronautical telemetry systems.

INTRODUCTION

The two-antenna problem in aeronautical mobile telemetry (AMT) comes about from the need to maintain constant connectivity between the transmit antenna of an airborne test article and a receiver ground station (see, e.g., [1]). If the test article is equipped with only one antenna, certain positions and flight maneuvers lead to blockage by the body of the test article. To allow the ground station to maintain constant connectivity with the test article, a second antenna is placed on the opposite side of the aircraft. In the case where the airborne test article is an airplane or fighter jet, these two antennas are placed on the bottom and top of the aircraft as pictured in Figure 1. This allows the ground station to maintain direct line of sight to at least one of the transmit antennas, independent of the test article's position relative to the ground station antenna.

The two-antenna problem arises from cases where both transmit antennas have direct line of sight with the ground station's receive antenna. In these cases, each of the two transmit antennas experience different delays to the ground station due to the variable distances between transmit antennas and the receive antenna as well as different channel responses. In some cases, these differences can cause deconstructive interference at the ground station, leading to poor receiver signal quality.

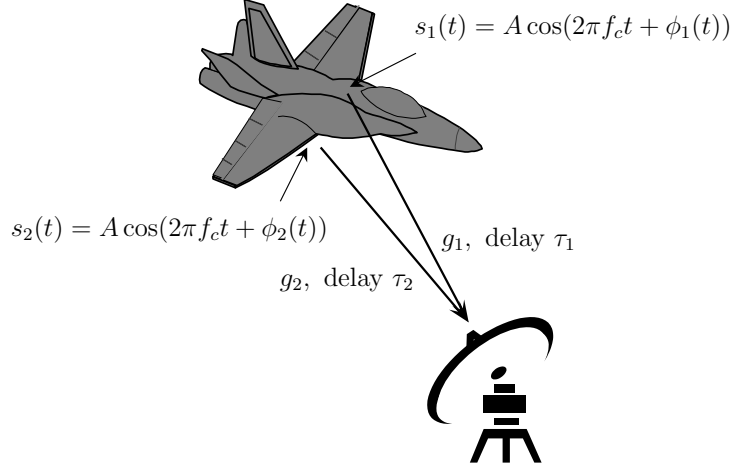


Figure 1: A system-level diagram describing the space-time coded ARTM CPM system.

Overcoming interference of this nature is called the two-antenna problem.

It has been shown that the two antenna problem can be solved using orthogonal space-time block codes [2, 3]. The work in [2] gives the solution in the case where the ARTM communication system uses the SOQPSK-TG waveform. The solution is based on the original Alamouti space-time codes (STC) from [4]. Only recently, this STC technique has been extended to the ARTM CPM waveform [5, 6], where it is also shown to solve the two-antenna problem. The extension from SOQPSK-TG to ARTM CPM is non-trivial.

The two-antenna problem leads to the scenario depicted in Figure 1, where the i th antenna transmits

$$s_i(t) = A \cos(2\pi f_c t + \phi_i(t)), \quad (1)$$

for $i = 1, 2$. Here, A is the amplifier gain applied to the waveform at the transmitter, f_c is the carrier frequency in Hertz, t is the traditional variable representing time, while $\phi_1(t)$ and $\phi_2(t)$ are the time-varying phase signals of the ARTM CPM waveform. Data are modulated onto these phase signals in the usual way (see, e.g., [7, 8]). The received signal at the ground station antenna can be modeled as

$$r(t) = g_1 A \cos(2\pi(f_c + \Delta f)(t - \tau_1) + \phi_1(t) + \gamma_1) + g_2 A \cos(2\pi(f_c + \Delta f)(t - \tau_2) + \phi_2(t) + \gamma_2) + n(t).$$

Here, g_1 and g_2 are the gains experienced by $s_1(t)$ and $s_2(t)$, respectively, as these signals are transmitted to the ground station. They represent the collective gains and losses accrued through the transmitter back end, the propagation channel, and the receiver front end, for each signal. The variable Δf is the frequency offset due to oscillator variability and Doppler shift. The delay variables τ_1 and τ_2 include all delays experienced by each of $s_1(t)$ and $s_2(t)$, respectively, through either cables or the propagation channels. The variables γ_1 and γ_2 are the phase shifts encountered by the respective $s_1(t)$ and $s_2(t)$ signals through the propagation channel. Finally, $n(t)$ is the thermal noise seen at the receiver, including such noise added to the signal by the receiver front-end components. This signal is modeled as a complex-valued zero-mean white Gaussian random process

pilot 1 128 bits	B1 8 bits	D1 840 bits	E1 8 bits	B2 8 bits	$\overline{D2}$ 840 bits	E2 8 bits	T1 8 bits
pilot 2 128 bits	B1 8 bits	D2 840 bits	E3 8 bits	B3 8 bits	$\overline{D1}$ 840 bits	E4 8 bits	T2 8 bits

Figure 2: Data format for a space-time coded transmitter. The top format is used by the first antenna, and the bottom format is used by the second antenna.

with power spectral density $2N_0$.

The STC-based solution to the ARTM CPM two-antenna problem requires optimal estimation of g_1 , g_2 , τ_1 , τ_2 , γ_1 , and γ_2 . To allow for optimal parameter estimation, a sequence of known pilot bits are transmitted within the data structure coming from each antenna (see Figure 2). We discuss these data structures at greater length in [6]. For this paper it suffices to say that the variance of the estimators for these parameters can be reduced, and even minimized, through proper design of the two 128-bit pilot bit sequences.

This paper addresses the problem of pilot bit-sequence design to enable optimal parameter estimation for the STC-based solution to the two-antenna problem using the ARTM CPM waveform. We provide the motivation and algorithm for choosing the sequences, and show that the Cramér-Rao lower bounds (CRLBs), which bound the variance of the estimators, are minimized by our specific pilot sequence selection. Such a design enables better performance in the actual implementation of the estimation algorithms. We also list both pilot sequences explicitly in this paper.

DESIGN APPROACH

Intuitively, since pilot 1 and pilot 2 are transmitted simultaneously and are used to allow the detector to do parameter estimation, we may assume that making the waveform associated with pilot 1 orthogonal to the waveform associated with pilot 2 is a reasonable approach to optimal pilot sequence design.

A. Cramér-Rao Lower Bounds

In this section, we argue that minimizing the Cramér-Rao lower bounds for estimators of g_1 , g_2 , γ_1 , and γ_2 is an equivalent problem to finding pilot sequences that produce orthogonal ARTM CPM waveforms (see [1] for additional details in the SOQPSK-TG case). Let $\mathfrak{g}_1 = g_1 e^{j\gamma_1}$ and $\mathfrak{g}_2 = g_2 e^{j\gamma_2}$. Note that we can optimize pilot sequences either in terms of the estimators for \mathfrak{g}_1 and \mathfrak{g}_2 , or the estimators for g_1 , g_2 , γ_1 , and γ_2 . We follow the approach from [1], and consider estimators for the real and imaginary parts of \mathfrak{g}_1 and \mathfrak{g}_2 . Thus, we still have four parameters to estimate.

Let \mathbf{p}_1 and \mathbf{p}_2 be column vectors obtained from sampling the ARTM CPM waveforms $s_1(t)$ and

$s_2(t)$ that are produced from the pilot 1 and pilot 2 sequences, respectively. (For our purposes, suppose that τ_1 and τ_2 are both zero. The estimators in [6] show how to find these parameters in general.) Samples are taken at $N = 4$ samples per symbol. Since ARTM CPM is a quaternary modulation scheme, and because the pilot sequences are 128 bits in length, then each of \mathbf{p}_1 and \mathbf{p}_2 are comprised of 256 complex-valued samples. We then define

$$\mathbf{P} = [\mathbf{p}_1 \quad \mathbf{p}_2], \quad (2)$$

and

$$\mathbb{P} = \begin{bmatrix} \Re\{\mathbf{P}\} & -\Im\{\mathbf{P}\} \\ \Im\{\mathbf{P}\} & \Re\{\mathbf{P}\} \end{bmatrix}, \quad (3)$$

where $\Re\{\cdot\}$ and $\Im\{\cdot\}$ are the real and imaginary operators. In [1] it is shown that the Fisher information matrix associated with estimating the four real-valued parameters $\Re\{g_i\}$ and $\Im\{g_i\}$ for $i = 1, 2$ is then simply

$$\mathbb{J} = \frac{1}{\sigma^2} \mathbb{P}^T \mathbb{P}, \quad (4)$$

where the variance of noise samples obtained by sampling $n(t)$ is $2\sigma^2$. The Cramér-Rao lower bounds for estimators of $\Re\{g_i\}$ and $\Im\{g_i\}$ for $i = 1, 2$, are then given by the diagonal elements of \mathbb{J}^{-1} . Note that the off-diagonal elements of \mathbb{J} contain combinations of sums of cross-correlations between the real and imaginary components of \mathbf{p}_1 and \mathbf{p}_2 . Also note that the diagonal elements of \mathbb{J} contain sums of auto-correlations between the real and imaginary components of \mathbf{p}_1 and \mathbf{p}_2 , which will be constant for all possible pilot sequences. Straightforward simulations can be used to show that minimizing the diagonal elements of \mathbb{J}^{-1} is best accomplished by making off-diagonal elements of \mathbb{J} as small as possible. We can achieve this if

$$\begin{aligned} \Re\{\mathbf{p}_1\}^T \Re\{\mathbf{p}_2\} &= \Re\{\mathbf{p}_1\}^T \Im\{\mathbf{p}_2\} \\ &= \Im\{\mathbf{p}_1\}^T \Re\{\mathbf{p}_2\} \\ &= \Im\{\mathbf{p}_1\}^T \Im\{\mathbf{p}_2\} = 0. \end{aligned} \quad (5)$$

Finally, it can be shown that if we simply find complex-valued \mathbf{p}_1 and \mathbf{p}_2 that are orthogonal (in the complex sense), i.e.,

$$\mathbf{p}_1^H \mathbf{p}_2 = 0, \quad (6)$$

then (except for in a few rare cases), we have achieved all cross-correlations in (5) to be zero as well. Thus, producing pilot sequences that satisfy (6) serves to minimize the Cramér-Rao lower bounds for the estimators of the complex channel gains.

B. Algorithm for Finding Pilot Sequences

At this point, we recognize that finding pilots that satisfy (6) may be impossible. Simply minimizing the magnitude of $\mathbf{p}_1^H \mathbf{p}_2$ will still, however, draw us close to our goal of optimal parameter estimation from the pilots.

Since each pilot sequence is 128 bits, we have $2^{256} \approx 1.16 \times 10^{77}$ possible ways to choose the pilots. Searching through this space of all possible sequences is completely impractical, as it

is approximately the same as the estimate of the total number of particles in the universe, the Eddington number, which is equal to 1.0×10^{80} . We propose a more efficient approach to finding good pilots as follows. Let us consider growing the pilot bit sequences eight bits at a time, always keeping the winning sequences from the previous iteration. We require 16 rounds of this algorithm to produce the desired length of 128 bits for both pilots. The approach is straightforward, in that we search through all 2^{16} possible additions to the current pilots, and keep the set of 16 bits (eight bits for each pilot) that minimize $|\mathbf{p}_1^H \mathbf{p}_2|$, where \mathbf{p}_1 and \mathbf{p}_2 represent the pilot samples up to and including the chunk under test. This requires us to calculate the samples for the ARTM CPM waveforms of each sequence from the saved bits in previous rounds of the algorithm with the possible additional bits appended to the ends. Each round of the process computes and compares $2^{16} = 65,536$ cross-correlations for a total of $2^{20} = 1,048,576$ correlation calculations in the entire algorithm. The process can be completed on a general purpose desktop computer in a few minutes.

C. Practical Considerations for the Pilot Sequences

Although the process outlined in the last section provides a mechanism to produce optimal (or nearly optimal) sequences by searching through a small selection of the total number of available possibilities, the final round of eight bits must actually be calculated in a new way. The detector for STC ARTM CPM waveforms is based on the Viterbi algorithm [5], and requires the waveform to be driven into a known and fixed state at the end of the pilot sequences so the detector can operate correctly on the remainder of the transmitted bits. Thus, the optimal solution is obtained through 16 rounds of selecting eight-bit chunks for each pilot sequence; however, the chosen pilots presented below are obtained using 15 rounds of the optimization algorithm, and the final eight bits are set to achieve the desired state. The interested reader is directed to [5] for the details.

RESULTS

The algorithms from the previous section were run to produce the following two 128-bit pilot sequences. The sequences are to be read from left to right, starting at the top row.

$$\begin{aligned} \text{pilot 1} = \{ & 0 \ 0 \ 0 \ 0 \ 1 \ 1 \ 0 \ 1 \ 1 \ 0 \ 0 \ 0 \ 0 \ 0 \ 0 \ 0 \\ & 0 \ 0 \ 1 \ 0 \ 0 \ 1 \ 0 \ 1 \ 0 \ 0 \ 1 \ 1 \ 1 \ 0 \ 1 \ 1 \\ & 1 \ 1 \ 0 \ 0 \ 0 \ 0 \ 1 \ 1 \ 0 \ 1 \ 0 \ 0 \ 1 \ 1 \ 0 \ 1 \\ & 1 \ 1 \ 0 \ 0 \ 1 \ 1 \ 0 \ 0 \ 1 \ 0 \ 0 \ 0 \ 1 \ 1 \ 0 \ 1 \\ & 1 \ 1 \ 1 \ 1 \ 1 \ 0 \ 1 \ 1 \ 1 \ 0 \ 0 \ 1 \ 1 \ 0 \ 0 \ 0 \\ & 1 \ 1 \ 1 \ 0 \ 1 \ 1 \ 1 \ 1 \ 1 \ 0 \ 1 \ 0 \ 1 \ 1 \ 1 \ 1 \\ & 1 \ 1 \ 0 \ 0 \ 1 \ 1 \ 0 \ 0 \ 1 \ 1 \ 1 \ 1 \ 1 \ 0 \ 1 \ 1 \\ & 1 \ 1 \ 1 \ 1 \ 1 \ 1 \ 1 \ 0 \ 1 \ 0 \ 0 \ 1 \ 0 \ 0 \ 0 \ 0 \}. \end{aligned}$$

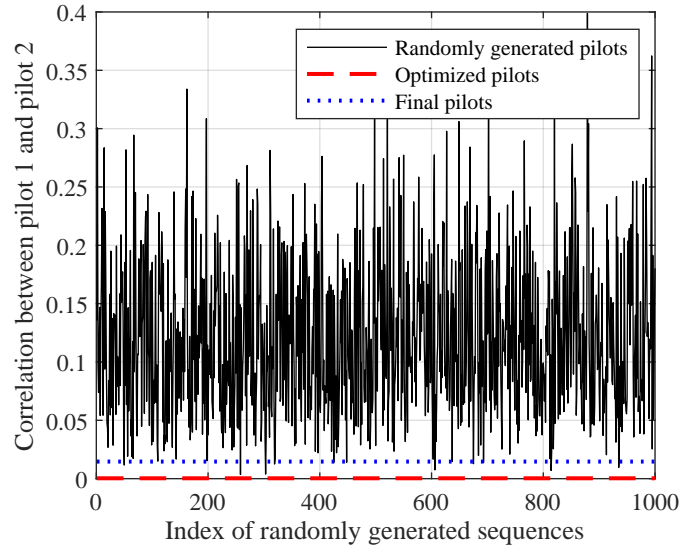


Figure 3: Cross-correlation parameters between pilot 1 and pilot 2 for the optimal sequences (red), the final sequences (blue), and 1000 randomly generated pilot pairs (black).

$$\text{pilot 2} = \{0 \ 1 \ 1 \ 0 \ 0 \ 1 \ 1 \ 1 \ 1 \ 1 \ 1 \ 0 \ 1 \ 1 \ 0 \ 0 \\
1 \ 0 \ 1 \ 0 \ 1 \ 1 \ 1 \ 0 \ 1 \ 1 \ 0 \ 0 \ 0 \ 1 \ 1 \ 0 \\
0 \ 0 \ 1 \ 0 \ 1 \ 1 \ 0 \ 0 \ 1 \ 0 \ 1 \ 1 \ 0 \ 1 \ 0 \ 1 \\
0 \ 1 \ 0 \ 0 \ 0 \ 1 \ 0 \ 0 \ 0 \ 0 \ 0 \ 0 \ 0 \ 1 \ 0 \ 1 \\
0 \ 1 \ 1 \ 1 \ 0 \ 0 \ 1 \ 1 \ 0 \ 0 \ 0 \ 1 \ 0 \ 0 \ 0 \ 0 \\
0 \ 1 \ 1 \ 0 \ 0 \ 1 \ 1 \ 1 \ 0 \ 0 \ 1 \ 0 \ 0 \ 1 \ 1 \ 1 \\
0 \ 1 \ 0 \ 0 \ 0 \ 1 \ 0 \ 0 \ 0 \ 1 \ 1 \ 1 \ 0 \ 0 \ 1 \ 1 \\
0 \ 1 \ 1 \ 1 \ 0 \ 1 \ 1 \ 0 \ 0 \ 1 \ 0 \ 0 \ 0 \ 0 \ 0 \ 0\}.$$

The last eight bits of each pilot sequence are specially designed for practical detector purposes, as mentioned in the previous section. Thus, we may expect the chosen sequences to be slightly suboptimal. Figure 3 shows the cross-correlation calculated as $|\mathbf{p}_1^H \mathbf{p}_2|$ for several sets of pilot sequences. The red-dotted line is the value obtained in the set of pilot sequences obtained if we were to run 16 rounds of the optimization algorithm. Since we could only run the optimization algorithm for 15 rounds and the final eight bits were fixed for practical decoder reasons, the actual pilot sequences given in this section only achieved the blue-dotted line. The black line shows the same metric for 1000 randomly generated pilot sequence pairs. Here we see that the chosen sequences are still very good, even with the practical requirements on the last eight bits of the pilots.

The Cramér-Rao lower bounds for the estimators corresponding to the complex-valued channel gains are shown in Figure 4 for all four channel gain parameters. Here we show the CRLBs corresponding to the final pilot sequences in red-dotted lines for all four cases. A set of 1000 randomly generated pilot sequences were also tested, and we note that even though fixing the last eight bits of each pilot seems to have affected the cross-correlation parameter slightly in Figure 3,

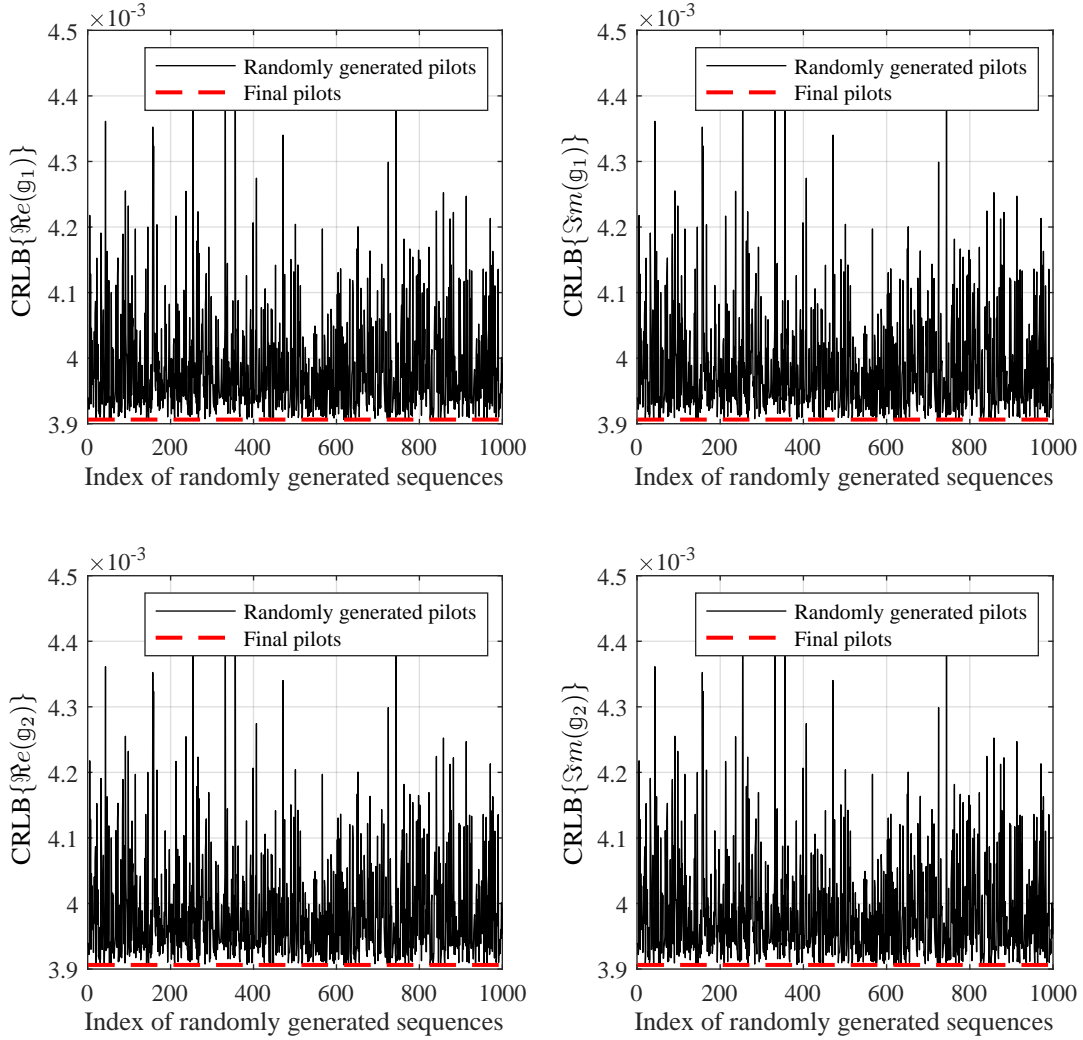


Figure 4: Cramér-Rao lower bounds for four channel gain parameters. The bounds are given for the pilots obtained and presented in this section in red, and 1000 randomly generated pilots are shown in black.

we do not seem to suffer any performance with regards to the CRLBs.

CONCLUSIONS

In this paper, we presented principles for finding pilot bit-sequences for optimal parameter estimation in STC ARTM CPM detectors. The pilots were presented explicitly, and they were shown to achieve the minimum (or nearly the minimum) CRLBs for the complex channel gain estimators. The pilots were constructed eight bits at a time, and allow for the convenience of setting the final eight bits of each pilot to allow the Viterbi-based detector to operate from a known state at the end of the pilot samples.

REFERENCES

- [1] M. Rice, J. Palmer, C. Lavin, and T. Nelson, “Space-time coding for aeronautical telemetry: Part I—estimators,” *IEEE Transactions on Aerospace and Electronic Systems*, vol. 53, no. 4, pp. 1709–1731, 2017.
- [2] M. A. Jensen, M. D. Rice, and A. L. Anderson, “Aeronautical telemetry using multiple-antenna transmitters,” *IEEE Transactions on Aerospace and Electronic Systems*, vol. 43, no. 1, pp. 262–272, 2007.
- [3] M. Jensen, M. Rice, T. Nelson, and A. Anderson, “Orthogonal dual-antenna transmit diversity for SOQPSK in aeronautical telemetry channels,” in *Proc. Int. Telemetry Conf. (ITC)*, (San Diego, CA), Oct. 2004.
- [4] S. Alamouti, “A simple transmit diversity technique for wireless communications,” *IEEE Journal on Selected Areas in Communications*, vol. 16, no. 8, pp. 1451–1458, 1998.
- [5] C. Josephson, E. Perrins, and M. Rice, “Space-time block-coded ARTM CPM for aeronautical mobile telemetry.” to appear in *IEEE Transactions on Aerospace and Electronic Systems*, 2021.
- [6] M. Rice, C. Josephson, W. Harrison, and S. Giddens, “On space-time coded ARTM CPM to solve the two-antenna problem,” in *Proc. Int. Telemetry Conf. (ITC)*, Oct. 2021.
- [7] E. Perrins and M. Rice, “Reduced-complexity detectors for multi-h CPM in aeronautical telemetry,” *IEEE Transactions on Aerospace and Electronic Systems*, vol. 43, no. 1, pp. 286–300, 2007.
- [8] Telemetry Group, “Telemetry standards,” standard, Range Commanders Council, White Sands, NM, July 2017.